The 5th European sCO_2 Conference for Energy Systems
March 14-16, 2023, Prague, Czech Republic

2023-sCO2.eu-132

THERMODYNAMIC ANALYSIS OF A REACTIVE PARTICLE-TO-SCO_2 HEAT EXCHANGER FOR RECOVERING STORED THERMOCHEMICAL ENERGY

Bryan J. Siefering*
The Pennsylvania State University
University Park, PA, USA
bjs6878@psu.edu

Muhammad Umer
The Pennsylvania State University
University Park, PA, USA

Ellen B. Stechel
Arizona State University
Tempe, AZ, USA

Brian M. Fronk
The Pennsylvania State University
University Park, PA, USA

ABSTRACT

The objective of this paper is to investigate the effect of off-design supercritical carbon dioxide (sCO_2) Brayton cycle operation on the thermodynamic performance of a heat exchanger/chemical reactor for transferring stored energy from hot, reduced, metal oxide particles into the power cycle. The device, termed an Energy Recovery Reactor (ERR), feeds gravity-driven particles through a bank of zigzag, finned, serpentine tubes containing sCO_2 flowing in counterflow to the particles. Preheated air introduced at the bottom of the reactor flows through the zig-zag channels also in counterflow with the particles and parallel flow with the sCO_2. The air supplies oxygen (O_2) as the reactant to drive exothermic re-oxidation of particles. The air also functions as a heat transfer medium between the energized particles and sCO_2.

In this study we develop a steady-state 1-D thermodynamic model of the ERR system. By defining controllable inputs such as inlet temperatures and flow rates of particles, air, and sCO_2, the remaining state points are calculated based on mass and energy balances. With set flow rates of particles, adjusting the sCO_2 cycle operating conditions (e.g., inlet temperature, flow rate, etc.) demonstrate how the performance of the ERR will change during off-design operation. Increasing the inlet temperature of the sCO_2 while maintaining the required outlet temperature results in a smaller temperature lift and decreases the heat duty of the system as a whole. When the system runs with a constant particle flow rate, the total amount of chemical heat available is constrained based on the redox reaction. Therefore, adjusting the heat transfer to the sCO_2 based on changes to the operating conditions results in changes to the recovery effectiveness and the ratio of sensible to chemical heat released by the particles. This model outputs the steady state operating conditions of the three domains within the reactor at various off-design conditions that are input to an existing segmented heat transfer model to calculate the temperature profiles and local heat transfer performance, which will be verified experimentally in future work.

INTRODUCTION AND BACKGROUND

The next generation of high temperature, central receiver concentrated solar power (CSP) systems are well suited for providing thermal energy to high efficiency power cycles using supercritical carbon dioxide (sCO_2) as the working fluid, [1]. The U.S. Department of Energy (DOE) has identified the recompression sCO_2 Brayton cycle as the most promising power cycle for coupling to next-generation, high temperature (>700°C) central receiver CSP systems due to the potential of higher cycle thermal efficiency than steam Rankine cycles. The sCO_2 power cycle also operates with a smaller physical size and higher power density, resulting in a less complex power block that can be implemented at lower capital costs, [2]. These power cycles operate at high pressure (~25 MPa) and require a turbine inlet temperature of >700°C to operate in the target efficiency window. Coupling an sCO_2 Brayton cycle to a CSP plant requires a high temperature heat transfer fluid to capture the thermal energy from the concentrated solar flux which is either sent to a thermal energy storage (TES) system or directly to the power cycle via a high temperature heat exchanger. In the U.S., three main types of high temperature heat transfer fluids are being investigated for third generation CSP systems: gas-phase, molten salt, and particles, [1].

The main benefit that concentrated solar thermal technologies have over other forms of intermittent renewable energy is the relative simplicity of large-scale thermal energy storage. While the thermal energy captured via one of the aforementioned heat transfer fluids in a solar receiver could be

* corresponding author(s)

DOI: 10.17185/duepublico/77309

used immediately to generate electricity via the power cycle, most systems incorporate thermal energy storage to enable continual energy output during periods of low solar resource. Most existing central receiver CSP systems using molten nitrate salt as both the heat transfer fluid in the receiver and the thermal storage medium. However, these salts tend to break down temperatures around 565°C, [1]. Thus, thermal storage technology for next-generation plants must be capable of storing and releasing energy at higher temperatures. For short term or daily storage, a common and inexpensive means of thermal energy storage is to use the sensible energy of the receiver heat transfer fluid itself, [3,4]. For high temperature CSP plants, this thermal storage includes the use of hot particles, [5], or higher temperature chloride molten salt, [6], stored for durations up to 18 hours, depending on the capacity of the TES system, [7].

Due to the high amount of recuperation in recompression sCO_2 Brayton cycles, the temperature lift through the primary heat exchanger is relatively small, ~200 K, [8]. Thus, when coupling this cycle to sensible thermal storage, large volumes are required. To reduce the size and cost of the storage tank while maintaining the stored energy content, the energy density of the storage media must be increased. This increase can be achieved by using a material with a higher specific heat capacity, though this approach comes at the cost of using a less developed and more expensive material. Another way to increase the energy density of the storage system while also releasing heat over a narrower range of temperatures is to store latent heat via a phase change material. However, these materials are often limited to lower temperatures and have low thermal conductivities, which leads to long charge/discharge rates, [4].

To address these challenges, the focus of this study is on coupling sCO_2 Brayton cycles to a system that stores energy through a combination of sensible heating and a reversible chemical reaction. An example of the system is shown in Figure 1. This practice is known as thermochemical energy storage (TCES). In this study, we consider the use of redox active metal oxide (MO_x) particles with diameters on the order of 300 µm. During system charging, the particles are sensibly heated and endothermically reduced in a low O_2 environment. When energy is required, sensible heat and the energy from an exothermic re-oxidation reaction can be transferred to heat sCO_2 from a temperature of approximately 550°C to 720°C. This process significantly increases the energy density of the stored material. For example, the enthalpy of reaction is 370 kJ kg^{-1} material at maximum extent of reduction for CAM28, the material considered in this study, [9]. TCES also potentially allows matching of the temperature at which exothermic energy is released with the temperature lift required for the sCO_2 cycle.

The use of MO_x particles for energy storage in an air-Brayton cycle was explored by Gorman *et al.,* [10]. In their work, the particles and the Brayton cycle working fluid (air) were directly mixed, exchanging both sensible and chemical energy. The heated, O_2 depleted air is the working fluid used directly in the Brayton cycle. They showed that in certain cases the air outlet (turbine inlet) temperature from their reactor could exceed the stored particle temperature due to the exothermic re-oxidation reaction. Other researchers have begun to explore different TCES materials and the coupling to power cycles, [10–15]. At present, there are no studies exploring the performance of the coupling reactor between the TCES system and the sCO_2 power cycle. Direct contact between stored particles and the working fluid is not possible for sCO_2 systems. Thus, this paper explores the performance of the Energy Recovery Reactor (ERR) when the coupled sCO_2 power cycle runs at off design conditions. Performance is evaluated using a steady state thermodynamic model where the operating conditions of the sCO_2 (inlet temperature, flow rate) are varied from their design values. The metric of performance is the effectiveness of recovery, a value

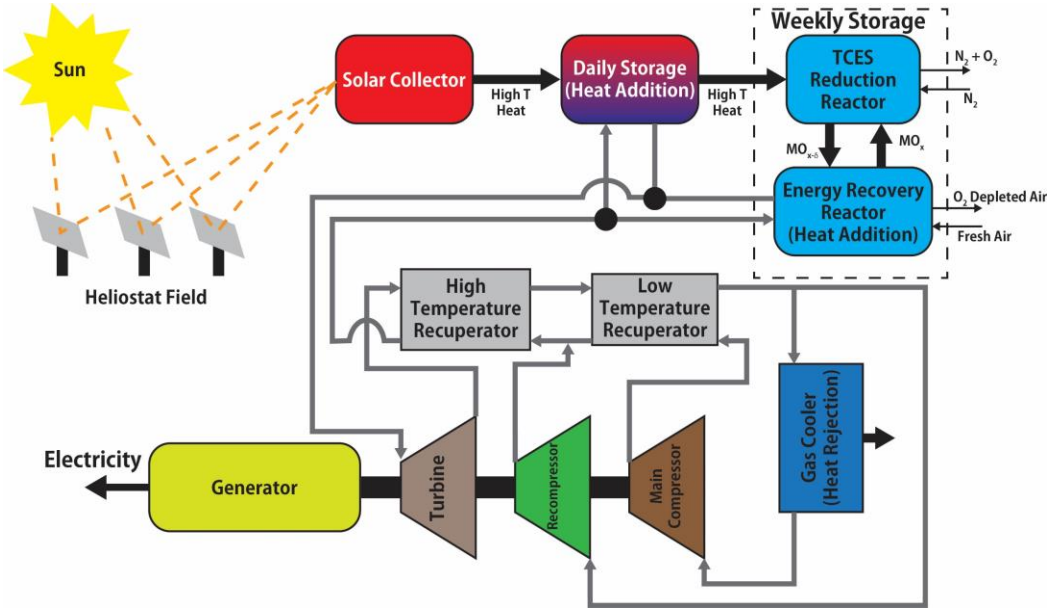

Figure 1: sCO_2 Brayton cycle with recompression coupled to CSP system with daily and weekly storage.

DOI: 10.17185/duepublico/77309

comparing how much energy transfers into the sCO_2 versus how much stored energy is supplied by the particles' sensible and chemical energy.

This model also compares the amount of energy recovered from the particles with how much is theoretically possible at the different off-design conditions. A complementing heat transfer model uses the conditions calculated in the thermodynamic model as inputs to calculate temperature profiles of the air, particles and sCO_2 through the reactor. It also calculates the local sensible and chemical energy release rates of the particles through the reactor height, which can be compared to the sensible energy change of the sCO_2 to again evaluate the effectiveness of recovery. These models are used to evaluate how off-design conditions of the sCO_2 Brayton cycle effect the performance of reactor coupling the power cycle and the TCES system.

ENERGY RECOVERY REACTOR SYSTEM DESIGN

Figure 1 shows a schematic of a concentrated solar power plant with TCES and an sCO_2 Brayton cycle. Our group has developed a novel device called the Energy Recovery Reactor (ERR) to couple the TCES system to a sCO_2 power cycle. Figure 2 shows conceptual rendering of the prototype scale ERR. This device serves as the primary heat exchanger in a recompression Brayton cycle. Within the device, both sensible and chemical energy are recovered by oxidizing the reduced TCES particles using near-ambient pressure air in counter flow. The air then transfers its energy via convection to the sCO_2 flowing through a bank of finned serpentine tubes through the body of the reactor. The wavy fins aid in heat transfer by increasing the heat transfer area of the sCO_2 circuit and increase the residence time to allow for complete oxidation of particles.

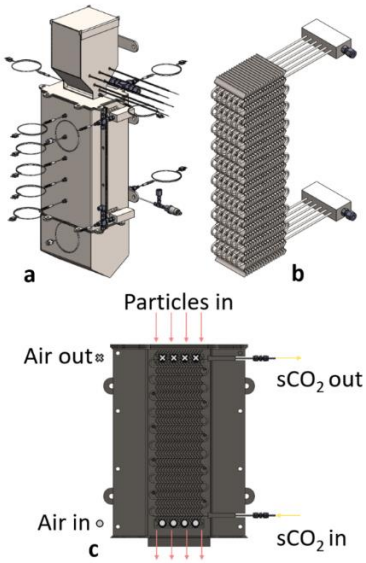

Figure 2: (a) Rendering of ERR prototype, (b) ERR heat exchanger core with wavy fins, (c) ERR fluid flow paths.

The reactor has three domains: MO_x particles, air, and sCO_2. The chemical equation used in the redox reaction is as follows:

$$\frac{1}{\delta}MO_{x-\delta} + O_2 \rightarrow \frac{1}{\delta}MO_x + \Delta H_{red}$$

Where δ is the reduction extent of the metal oxide particles. The particles transfer sensible and chemical energy primarily to the air via convection, though at the high temperature, radiation effects become important.

As shown in Figure 3, the inputs to the ERR system are fresh air, hot reduced MO_x particles, and sCO_2 returning from the power block. The ERR has been developed to recover the stored sensible and chemical energy of the particles at a high recovery efficiency, however because the reactor behaves as a counterflow heat exchanger between the particle and air, the air leaving the system carries away a large amount of sensible energy. To reduce this potential parasitic, within the system recuperation and recirculation are used to recover the exiting energy and preheat the incoming ambient fresh air. The air domain of the ERR must operate as an open cycle because the O_2 within the air is consumed by the particles during re-oxidation, thus limiting the ability to continually recirculate.

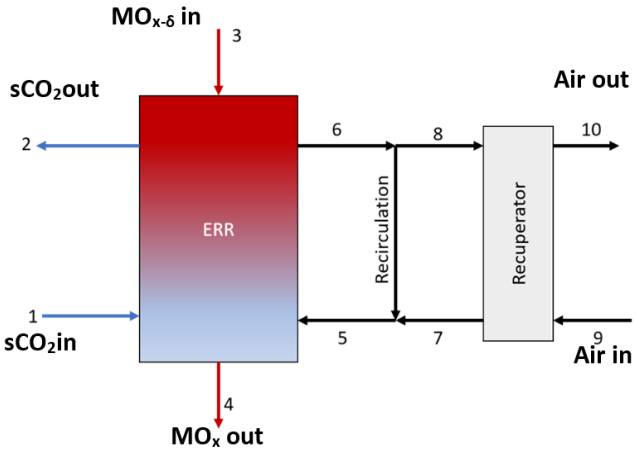

Figure 3: Flow schematic of ERR with recirculation and recuperation.

THERMODYNAMIC MODEL DEVELOPMENT

A black-box thermodynamic state point model has been developed in *Engineering Equation Solver* (EES), [16] to study the steady state operating conditions of the ERR. The model calculates the required flow rate of air to completely oxidize all particles and the conditions at each state points in Figure 3 using energy and mass balances. The required model inputs are inlet temperatures of the particles (State 3), air (State 9), and sCO_2 (State 1) and flow rates of particles and sCO_2. These results can be used to evaluate the recovery effectiveness (Eq. 1).

A mass balance is used to determine the amount of O_2 required to fully re-oxidize the $MO_{x-\delta}$ particles while in the ERR. The amount of O_2 needed relates directly to the off-stoichiometric δ of the stored, incoming particles. From the assumed inlet δ and the molar flow rate of particles, the flow rate of O_2 that is consumed by the particles during the re-oxidation reaction is calculated using Equation 1.

DOI: 10.17185/duepublico/77309

$$\dot{n}_{O_2,consumed} = \frac{\delta}{2}\dot{n}_{MOx} \quad (1)$$

At steady state stoichiometric conditions, the air stream leaving the reactor is completely depleted of O_2, thus the air cannot be fully recirculated through the system without the introduction of fresh air, requiring the air domain of the ERR to operate as an open loop. In this study, a theoretical air percentage of 101% is used, which ensures that there is always excess oxygen to drive the reaction. To calculate the air flow rate that enters the ERR, the molar flow rate of O_2 consumed is converted into mass flow rate through the molecular weight of O_2. The flow rate of O_2 entering the reactor at state point 5 is the product of the consumed O_2 mass flow rate and the theoretical air percentage value, assumed constant at 101% in this study. With this value defined, an energy balance and mass around the recirculation system is used to solve the required flow rate of fresh air that must be brought into the system depending on the amount recirculated to keep the air oxygenated to fully re-oxidize the particles.

With all the flow rates defined and either the outlet temperature of sCO_2 or heat transfer rate into the sCO_2 specified, an energy balance is used to solve the individual state point temperatures and flow rates by solving a system of equations (Eq. 1 – Eq. 4). Equation 2 is the energy balance used in the model to couple all three domains of the ERR.

$$\Delta\dot{H}_{sCO_2} = \Delta\dot{H}_{MO_x,chem} + \Delta\dot{H}_{MO_x,sens} + \Delta\dot{H}_{N_2} + \Delta\dot{H}_{O_2} \quad (2)$$

The enthalpy change of the sCO_2 on the left-hand side of the equation is specified by either directly setting the desired thermal output of the ERR or setting the required outlet temperature and mass flow rate for the sCO_2 cycle. In this study, we consider the baseline design of a 1 kW_{th} ERR prototype that heats sCO_2 from 550°C to 720°C. For these conditions, the sCO_2 flow rate is then calculated.

The energy addition from the chemical reaction is the product of the consumed O_2 and the enthalpy of reaction, represented in Equation 3.

$$\Delta\dot{H}_{MO_x,chem} = \dot{n}_{O_2,consumed} H_{rxn} \quad (3)$$

The TCES material used in this model is a doped calcium manganite perovskite denoted as CAM28. Babiniec *et al.*, reported in [9], that CAM28 has a reduction enthalpy of 320 kJ mol O_2^{-1} when reduced to a δ of ~0.3. Miller *et al.* developed a thermodynamic model to further relate the equilibrium δ as a function of the temperature and partial pressure of O_2 in [17]. With this material, the reaction enthalpy extraction is possible at temperatures up to 1250°C, enabling larger energy storage densities through sensible recovery by storing the particles at higher temperatures, [9]. The sensible energy recovery of the particles is shown in Equation 4.

$$\Delta\dot{H}_{MO_x,sens} = \dot{m}_p \bar{c}_{p_p}\left(T_{p,in} - T_{p,out}\right) \quad (4)$$

The last two enthalpy terms in Equation 2 are the sensible parasitic losses from O_2 and N_2 in the system. The contribution of O_2 to the parasitic is very minimal as the only O_2 that removes energy from the system is from the excess air provided through the theoretical air percentage. The N_2 in the air does not react and absorbs heat from the particles during the process of flowing through the ERR. Heat transfers to the sCO_2 during this process, however even after recirculation and recuperation the outlet air, containing mostly N_2, leaves at an elevated temperature compared to the inlet and therefore contributes to parasitic loss. There are no parasitic losses accounted for in the model from heat loss from of the ERR. It is assumed to be a perfectly insulated system.

The performance of the Energy Recovery Reactor system is evaluated using an energy recovery effectiveness defined above in Equation 5. The recovery effectiveness is the amount of energy put into the sCO_2 compared to how much stored energy is recovered from the particles sensibly and chemically. As shown by the energy balance in Equation 2, the only parasitic of this system come from energy leaving the system via a flow.

$$\eta_{recovery} = \frac{\Delta H_{sCO_2}}{\Delta H_{MO_x,sens} + \Delta H_{MO_x,chem}} \quad (5)$$

Because the sCO_2 enters the ERR nominally at 550°C, the counterflow air temperature should enter the system at or above that temperature to ensure that all the energy from the particles is going towards heating the sCO_2, and that the air isn't removing initially cooling the sCO_2 when it first enters the reactor chamber. Therefore, the air temperature entering the reactor chamber is constrained in the model at 550°C. In practice, this temperature would be achieved via a combination of recirculation and recuperation, as shown in Figure 3. This value also defines the minimum temperature the particles can leave exit the system and ties it to the inlet temperature of the sCO_2. To evaluate the amount of energy removed from the particles versus the total amount of energy available for removal. Equation 6 defines an additional performance quantifier.

$$\eta_{recovery,potential} = \frac{\Delta H_{MO_x,sens} + \Delta H_{MO_x,chem}}{\Delta H_{MO_x,sens,max} + \Delta H_{MO_x,chem}} \quad (6)$$

The maximum particle sensible energy in this equation is calculated from Equation 5, where the particle outlet temperature is set to the inlet temperature of the sCO_2.

These criteria are used in the thermodynamic model to evaluate the off-design performance of the ERR when coupled to an sCO_2 Brayton cycle. By modifying particle and sCO_2 flow rates, and sCO_2 inlet temperature and heat duty, the changes in recovery effectiveness and sensible heat recovery potential describe the performance of the ERR at steady state.

DOI: 10.17185/duepublico/77309

HEAT TRANSFER MODEL DEVELOPMENT

To complement the thermodynamic model, a 1-D segmented heat transfer model has been developed to evaluate the local temperature distributions and heat transfer rates within the reactor for a given physical geometry. This model enables the identification of pinch points and locations where exothermic reactions were not possible due to insufficient O_2 or temperature. In this model, it is assumed the particles only transfer energy into the air via convection, which then subsequently transfers the heat into the sCO_2 loop. Radiation and conduction from the dilute particle flow directly to the wall are not considered. These effects will be considered in a future study. The full reactor domain is set based on the geometry of the ERR. The domain is segmented in the flow direction of air/particles. Each segment has an equal non-dimensional height of *dx*, determined by the total number of nodes *N* and the reactor physical height. In this work, the total height of the reactor is 16 inches and 300 nodes are used to discretize the domain. Grid independence was tested by running the model with various numbers of nodes and found that the model operated independently of the number of nodes used. This is because the model is heavily based on a resistance network that is not sensitive to mesh size. The heat transfer area of the sCO_2 domain is determined from the total length of tubing used in the heat exchanger core and the tube inside and outside diameter in addition to the surface are enhancement provided by the wavy fins. The tube diameter used in this study is 1/8 inch outside diameter with a 0.028 inch wall thickness. The fin surface area is calculated by taking the product of the total unbent length of a fin and the width of the fin, in this case 3 inches. Figure 4 displays the discretized domain, overlaid on a cross section of the ERR showing the flow directions of the particles, air, and sCO_2.

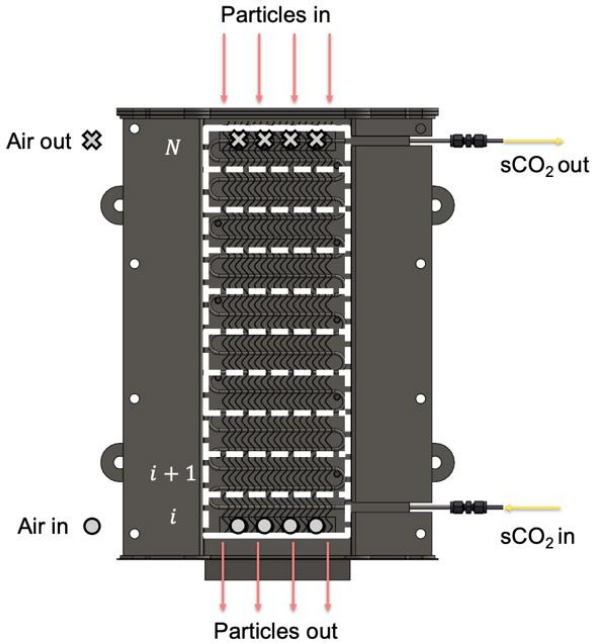

Figure 4: Discretized domain of ERR and flow directions.

The general transport equation is used to create an energy balance for the three flow domains within each segment, each treated as a control volume. Figure 5 shows the heat transfer taking place within each of the control volumes. This control volume segment provides a visual representation of the modes of energy exchange within each segment. The reduced general transport equation energy balances are shown in Equations 7-9.

$$\dot{m}_{CO_2} c_{p_{CO_i}} \left(T_{CO_{2i+1}} - T_{CO_{2i}}\right) = \frac{UA}{N}\left[T_{Air_i} - T_{CO_{2i}}\right] \quad (7)$$

$$\dot{m}_{Air} c_{p_{Air_i}} \left(T_{Air_i} - T_{Air_{i+1}}\right) = -\frac{UA}{N}\left[T_{Air_i} - T_{CO_{2i}}\right] + \frac{h_{a,p,i} A_p}{N}\left[T_{p_i} - T_{Air_i}\right] \quad (8)$$

$$\dot{m}_p c_{p_p} \left(T_{p_i} - T_{p_{i+1}}\right) = \frac{h_{a,p,i}\, A_p}{N}\left[T_{p_i} - T_{Air_i}\right] - \Delta H_{rxn}\, \dot{n}_{O_2\ consumed} \quad (9)$$

The overall conductance (*UA*) of the heat exchanger is calculated within the model based on the geometry of the ERR heat exchanger and the input flow rates. It is comprised of the resistances from convection between the air and tube, conduction through the tube and convection of sCO_2 in the tube. The correlation used for air to heat exchanger core convection is the Zukauskas correlation for flow over a bank of in-line tubes [18]. Additionally, the internal flow convection of the sCO_2 is estimated using the Dittus-Boelter correlation for fully developed internal turbulent flow in a tube [19]. The value of each of the thermophysical property used in the evaluation of the conductance or energy balance equations is calculated locally using the CoolProp Python package, based on the temperature and pressure within the specific node [20].

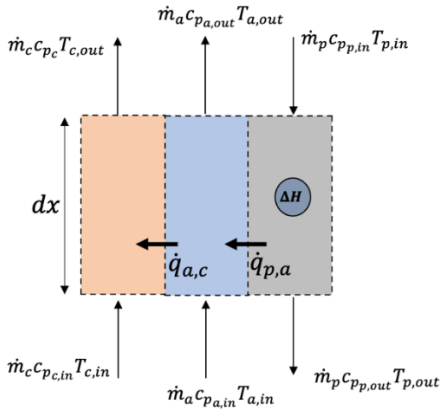

Figure 5: Control volume of heat transfer within ERR.

Convection heat transfer between the particles and air is calculated from a Nusselt number correlation for flow past a

DOI: 10.17185/duepublico/77309

single sphere, from Whitaker [21]. The total particle heat transfer area is a function of the residence time and particle flow rate. These two values are used to calculate the total number of particles within the reactor. An assumption is made that the particles are evenly distributed within the reactor, and thus the total surface area of particles, calculated from the product of the number of particles and a single particle surface area, a function of the particle diameter, is evenly distributed among the segmented control volumes.

The heat transfer model accounts for the chemical energy release by evaluating δ at thermodynamic equilibrium. A molar balance subfunction within the model takes the particle temperature, the local O_2 and N_2 mole fraction in the air stream, the molar flow rate of O_2 and the δ of the particle coming into the control volume. It then evaluates what the equilibrium δ of the particle should be based on the temperature and partial pressure of O_2, using the thermodynamic modeling fit from Miller *et al.* in [17]. A change in the δ then can be related to the amount of O_2 consumed in the node, and then further related to the heat release through the exothermic enthalpy of reaction. The sub function outputs new values for δ, and the mole fractions and molar flow rate of O_2 to be used as inputs for the next segment. The heat released through the exotherm contributes to the particle temperature as shown in Equation 9.

Because the ERR behaves as a counterflow heat exchanger, a minimization approach is needed to solve the outlet temperature of the particles. The Euler method is used to calculate the temperature of each domain in each control volume, starting with the inlet of sCO_2 and air and outlet of particles. Because the inlet temperature of particles is a controllable variable, it is set and a guess value for the outlet temperature is made. A minimization function within the SciPy [22] package of Python is used to iterate the particle outlet temperatures until the results of the Euler method calculation produces a result within the convergence criteria, set at 1°C.

In addition to the local temperature profiles, the model calculates the local heat transfer rate through the reactor within each control volume. The sensible heat release rate by the particles in an individual segment is calculated from the product of the particle mass flow rate, specific heat capacity and the temperature difference through the node. Likewise, the local chemical heat transfer rate is calculated using the product of the O_2 consumed within a segment, found from the molar balance subfunction, and the enthalpy of reaction. Summing the local chemical and sensible heat release rates at all nodes results in a total heat release rate by the particles which can be used in a recovery effectiveness equation, like Equation 5. A cumulative sum of the heat transfer rate into the sCO_2 is also done using the flow rate and change in specific enthalpy across an individual node. Similar to the thermodynamic model, the heat transfer model does not include heat losses to the environment.

THERMDOYNAMIC MODEL RESULTS

To perform parametric analyses on the steady state thermodynamic model, the model must be fully defined. This constraint results in some fixed parameters during the study. All of the controllable inputs to the model are set as fixed values except those studied in the parametric analysis. Table 1 shows a list of the constrained values within the model. These values were chosen based on the storage condition of the particles and expected performance of the sCO_2 Brayton cycle. The inlet air temperature is defined at 550°C in the system to ensure that the air is not removing energy from the sCO_2 cycle during operation. This is one of the ways the off-design operation the sCO_2 cycle impacts the performance of the ERR system. The recirculation percentage of 75% was chosen to increase the air velocity within the ERR without adding additional O_2. The effectiveness of the recuperator was chosen based on an estimate for a small commercially available recuperator.

Table 1: Fixed parameters in steady state thermodynamic model.

Variable	Value [Units]
δ	0.2 [-]
ΔH_{rxn}	320 [kJ mol O_2^{-1}]
Theoretical Air Percentage	101 [%]
$T_{p,in,3}$	1000 [°C]
$T_{a,in,5}$	550 [°C]
$T_{a,in,9}$	25 [°C]
P_{sCO_2}	25 [MPa]
ε	0.5 [-]
Recirculation Percentage	75 [%]

The thermodynamic model is used to evaluate the effect of different inlet sCO_2 operating conditions on the ERR performance via a parametric analysis. The range of conditions are representative of sCO_2 Brayton cycle off-design operation. Figure 6 shows the variation of sCO_2 inlet temperature ± 100 K from the design temperature of 550°C at two different particle mass flow rates. The air mass flow rates for these studies calculated from the model were 0.57 g s^{-1} and 0.97 g s^{-1} for the respective particle flow rates of 1.75 g s^{-1} and 3 g s^{-1}. As shown,

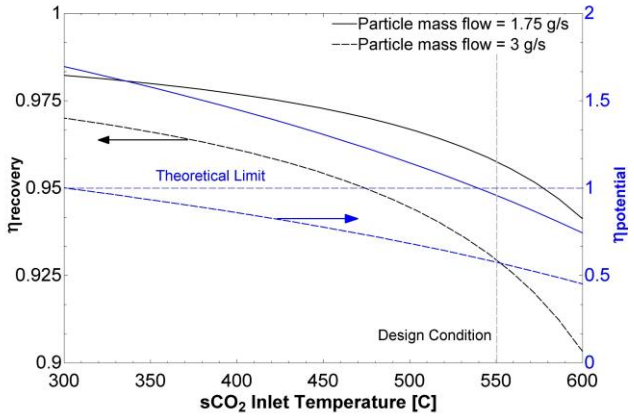

Figure 6: Thermodynamic model results for various sCO_2 inlet temperatures *versus* recovery effectiveness and potential.

DOI: 10.17185/duepublico/77309

the recovery effectiveness of the system increases as the temperature drops below the design condition for both particle flow rates. Because the flow rate of sCO_2 is fixed in this study (4.644 g/s for 1 kW at design temperatures), decreasing the inlet temperature while maintaining the outlet temperature at the design value of 720°C increases the required heat duty of the ERR.

Because the flow rate of particles is fixed, the amount of chemical energy potentially released by the particles is also fixed (assuming complete re-oxidation), and therefore if more heat is required to transfer into the sCO_2 the particles must release more sensible heat in the process. For given flow rates of particles and sCO_2, 1.0 is the maximum theoretical value for the potential energy recovery, defined previously in Equation 6. This limit is where the particle outlet temperature is equal to the sCO_2 inlet temperature, and the particles have been completely oxidized. The right axis of Figure 6 shows how this value changes with inlet temperature of sCO_2. In the case of the sCO_2 flow rate used in this study, the theoretical maximum limit for the recovery potential occurs at sCO_2 inlet temperature of 539°C and 302°C for the 1.75 and 3 g s^{-1} particle flow rates respectively.

Figure 7 shows that as the sCO_2 inlet temperature rises, and thus the required heat duty decreases, the sensible ratio, defined in Equation 10, decreases as the heat needed for heating sCO_2 provided by the particles comes primarily from re-oxidation, especially at higher flow rates of particles.

$$Sensible\ Ratio = \frac{\Delta H_{MO_x,sens}}{\Delta H_{MO_x,sens} + \Delta H_{MO_x,chem}} \quad (10)$$

A key takeaway from these results is that the mass flow rate of particles must be controlled as the required heat duty of the system changes to maximize recovery effectiveness. If the inlet sCO_2 temperature increases above the design value, the particle mass flow rate must be decreased to utilize more of the sensible energy available.

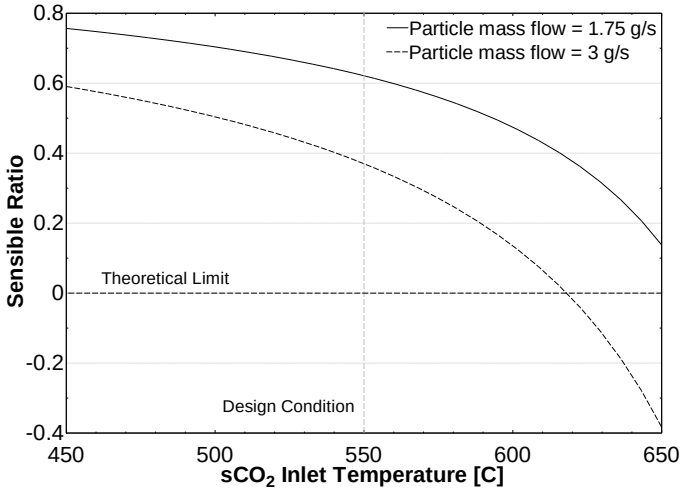

Figure 7: sCO_2 inlet temperature versus sensible heat ratio for fixed sCO_2 mass flow and outlet temperature.

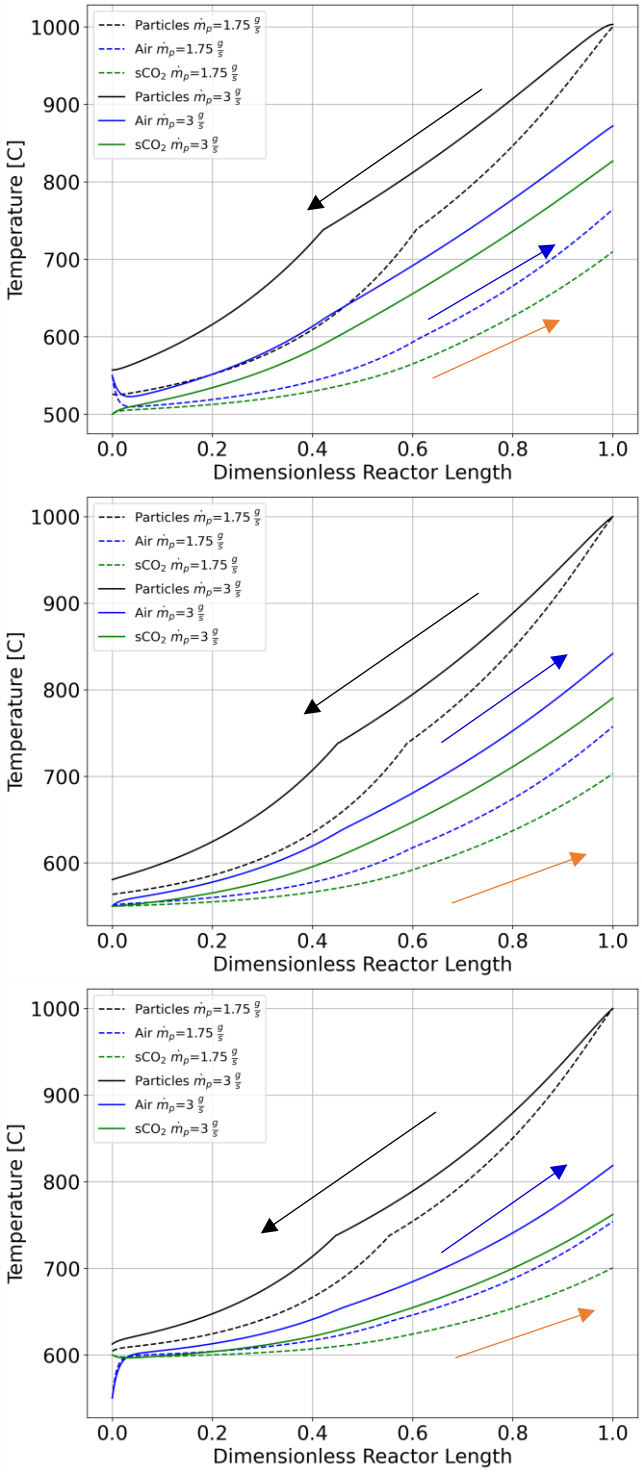

Figure 8: Heat transfer model results for ERR temperature profiles with sCO_2 inlet temperature of (top) 500°C (middle) 550°C (bottom) 600°C.

With fixed temperatures of the sCO_2 at their design values, and changing flow rates of sCO_2, similar trends to the results shown in Figure 6 and Figure 7 can be observed. As the flow rate

DOI: 10.17185/duepublico/77309

decreases, the heat duty of the system decreases and at a fixed particle flow rate the amount of heat available from the particles is used at various effectiveness depending on the change in operating condition. This model can be used to gain insight on how the flows of the other domains within the ERR must be adjusted if the sCO_2 Brayton cycle coupled to the ERR is operating off design conditions.

HEAT TRANSFER MODEL RESULTS

The 1-D segmented heat transfer model calculates the temperature profiles and local heat transfer rates through the reactor. Steady state operation is again assumed in this model, however the only constraints in this model are on the inlet conditions and reactor physical geometry (e.g., height, heat transfer area, etc.).

Unlike the thermodynamic model, the sCO_2 outlet temperature and heat duty are calculated, and therefore change based on inlet conditions. Using the same particle flow rates investigated in the thermodynamic model parametric study, the off-design inlet conditions of sCO_2 are investigated for conditions both above and below the design conditions.

Figure 8 shows the temperature profiles of the ERR operating at two particle flow rates (1.75 g/s, 3 g/s) and three sCO_2 inlet temperatures, (500°C, 550°C, 600°C). The arrows indicate the flow direction of each domain. As expected, for each of the sCO_2 inlet temperatures, the temperature lift of sCO_2 is less at the lower particle flow rate. This trend is due to less available total energy within the system, both chemical and sensible. As the sCO_2 inlet temperature increases, at a particle flow rate of 3 g/s, the outlet temperature of sCO_2 decreases because the inlet temperature of air is again constrained to 550°C, and therefore heat does not immediately transfer into the sCO_2 from the air, rather the sCO_2 is initially cooled by the air. The inlet sCO_2 temperature has a major impact on the convective heat transfer between the air and the sCO_2 because of varying temperature differences between the two domains. The particles reacting in the air flow allow the air to behave like a fluid with an infinite heat capacity, hence why the temperature can climb even while energy is transferring to the sCO_2.

The total heat release rate from the particles within the ERR for the design condition case is 1016 W and 1705 W for 1.75 and 3 g s^{-1} particle flow rates respectively. Increasing the sCO_2 inlet temperature to 600°C results in a 5.8% increase for the 1.75 g s^{-1} case and 4.0% increase for 3 g s^{-1}. Decreasing sCO_2 inlet temperature to 550°C decreases the total heat release rate by 6.1% and 5.1% for the particle flow rates respectively. However, similar to the thermodynamic model, increasing the particle flow rate does have a significant impact on the total heat released by the particles. The total amount of chemical heat is a function of the particle flow rate, and thus it is uniform in each varying temperature run, around 343 W for the 1.75 g s^{-1} case and 597 W for the 3 g s^{-1}. Figure 9 shows the cumulative heat release rate through the length of the reactor. The particles do not begin reacting until they reach a temperature and partial pressure of O_2 where the exothermic reaction can move forward based on the local reduction extent. When they are introduced into the reactor at the top, they require O_2 to undergo reaction.

Depending on inlet conditions, there may be zero O_2 at the exit of the air stream, which is the same location as the inlet of

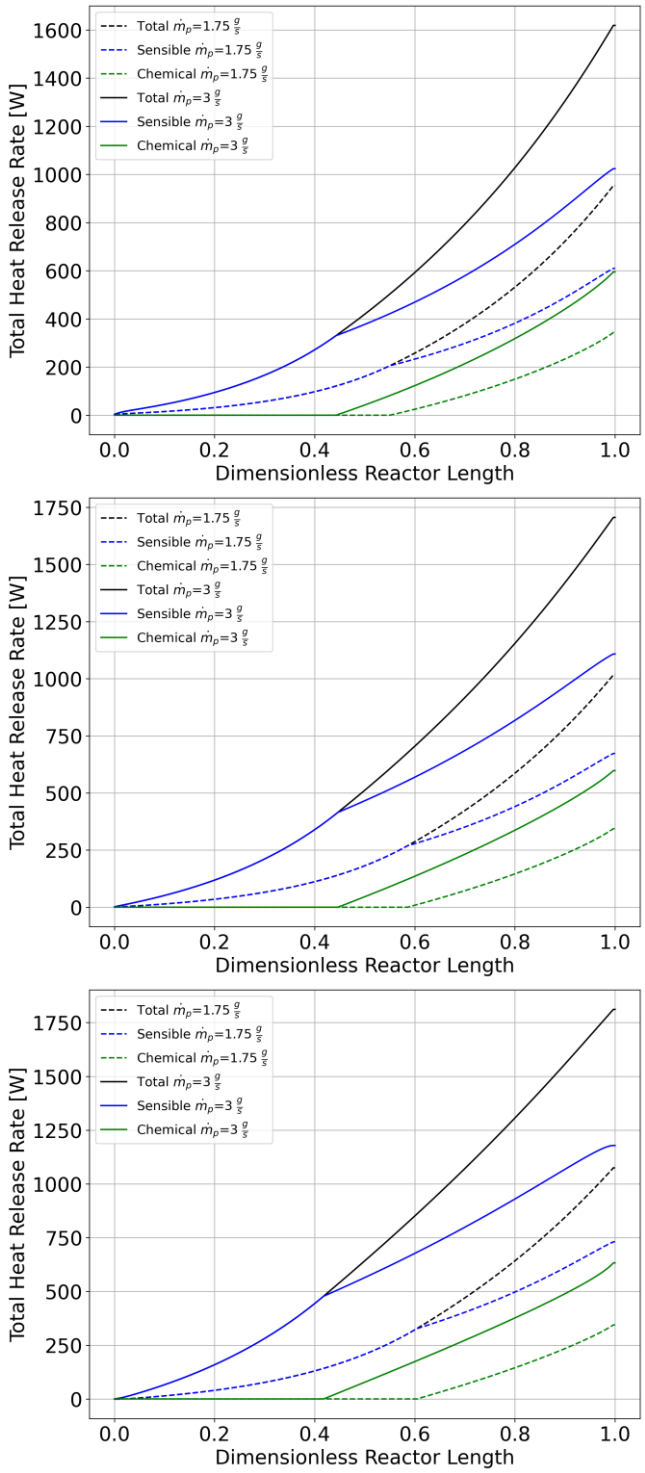

Figure 9: Heat transfer model results for ERR heat release rate profiles with sCO_2 inlet temperature of (top) 500°C (middle) 550°C (bottom) 600°C.

DOI: 10.17185/duepublico/77309

the particle stream. The particles will then remain reduced until they encounter sufficient O_2 to begin the exothermic reaction. The reaction proceeds while the local particle temperature and environment partial pressure of O_2 are satisfactory to carry the reaction forward. Uniform chemical heat release is desired as then the particles are providing the condition where the air acts as a quasi-infinite capacitance fluid and can maintain a larger temperature difference between the air and sCO_2. The increased sCO_2 inlet temperature allows for the particles to remain in the equilibrium conditions for longer, and therefore reduces the need for sensible energy in this region, indicated by the change in slope when the chemical reaction begins. This trend is shown in the plots as the sCO_2 inlet temperature is increased, the cumulative sensible heat release rate is lower, and the chemical heat release begins at a lower dimensionless reactor length.

CONCLUSIONS

This paper investigated the effects of operating an sCO_2 Brayton cycle at off-design conditions on the performance of the coupling device between a TCES system and the power cycle. A steady state thermodynamic model has been developed to determine the recovery effectiveness and potential, as well as the sensible-to-chemical energy ratio over a variety of sCO_2 inlet temperature conditions. A complementing 1-D segmented heat transfer model calculated the temperature profiles and cumulative heat release rates through the reactor at various particle flow rates and sCO_2 inlet temperatures. The following observations can be made about the Energy Recovery Reactor system when operating at off-design conditions:

- Because the ERR utilizes both chemical and sensible energy to heat the sCO_2, increasing the particle flow rate does not linearly increase the energy into the sCO_2 due to ratio of sensible and chemical heat release changing with particle flow rate
- As the sCO_2 inlet temperature increases, recovery effectiveness decreases from increased parasitic loses flowing out of the reactor and recovery potential decreases from not utilizing all the sensible energy available in the particles and relying more on chemical energy
- If other operating conditions (particle flow rate, air inlet temperature) are not changed with variances in the sCO_2 flow conditions, the system effectiveness decreases and target conditions will not be met

Understanding the implications of running an sCO_2 Brayton cycle at off design conditions on a device used to add heat to the system is important as any changes can lead to inefficiencies or failures. The thermodynamic and heat transfer models developed in this study mimic steady state operating conditions, so transient effects are not represented in this work. Future work will investigate the transient effects of changing these flow conditions. These two models also assume a fixed air inlet temperature set to match the design condition for sCO_2. This assumption is appropriate because the experimental setup associated with this work uses inline air heaters to preheat the air to the desired temperature, so off design effects in the sCO_2 loop will not affect the inlet temperature of air as they are controlled by separate systems. Future work will use this experimental setup to validate the model-based results. Finally, the results of these models can serve as the basis for model-based control of particle flow rates as power cycle conditions change.

NOMENCLATURE

c_p	Specific heat capacity [J kg^{-1} K^{-1}]
dx	Non-dimensional control volume height [-]
H_{rxn}	Reaction enthalpy [J kmol^{-1}]
h	Convective heat transfer coefficient [W m^{-2} K^{-1}]
$\dot{m}$	Mass flow rate [kg s^{-1}]
N	Total number of nodes [-]
T	Temperature [K]
UA	Heat exchanger conductance [W K^{-1}]

Greek

δ	Reduction extent
ε	Recuperator effectiveness
η	Effectiveness

Subscripts

a	Air
c	sCO_2
i	Current node
MO_x	Metal oxide particles
p	Particle

ACKNOWLEDGEMENTS

This material is based upon work supported by the U.S. Department of Energy's Office of Energy Efficiency and Renewable Energy (EERE) under the Solar Energy Technologies Office Award Number DE-EE0008991. The views expressed herein do not necessarily represent the views of the U.S. Department of Energy or the United States Government. We also gratefully acknowledge Drs. Ivan Ermanoski, Ryan Milcarek, and Arindam Dasgupta and the rest of the project team for helpful conversations.

DOI: 10.17185/duepublico/77309

REFERENCES

[1] Mehos, M., Turchi, C., Vidal, J., Wagner, M., Ma, Z., Ho, C., Kolb, W., Andraka, C., and Kruizenga, A., 2017, *Concentrating Solar Power Gen3 Demonstration Roadmap*.

[2] Turchi, C. S., Ma, Z., Neises, T. W., and Wagner, M. J., 2013, "Thermodynamic Study of Advanced Supercritical Carbon Dioxide Power Cycles for Concentrating Solar Power Systems," Journal of Solar Energy Engineering, Transactions of the ASME, **135**(4), pp. 1–7.

[3] Gil, A., Medrano, M., Martorell, I., Lázaro, A., Dolado, P., Zalba, B., and Cabeza, L. F., 2010, "State of the Art on High Temperature Thermal Energy Storage for Power Generation. Part 1-Concepts, Materials and Modellization," Renewable and Sustainable Energy Reviews, **14**(1), pp. 31–55.

[4] Evans, A., Strezov, V., and Evans, T. J., 2012, "Assessment of Utility Energy Storage Options for Increased Renewable Energy Penetration," Renewable and Sustainable Energy Reviews, **16**(6), pp. 4141–4147.

[5] Ho, C. K., 2016, "A Review of High-Temperature Particle Receivers for Concentrating Solar Power," Appl Therm Eng, **109**, pp. 958–969.

[6] Ding, W., and Bauer, T., 2021, "Progress in Research and Development of Molten Chloride Salt Technology for Next Generation Concentrated Solar Power Plants," Engineering, **7**(3), pp. 334–347.

[7] Thonig, R., and Lillliestam Richard, 2022, *CSP Projects Around the World*.

[8] Brun, K., Friedman, P., and Dennis, R., eds., 2017, *Fundamentals and Applications of Supercritical Carbon Dioxide (SCO_2) Based Power Cycles*, Woodhead Publishing.

[9] Babiniec, S. M., Coker, E. N., Miller, J. E., and Ambrosini, A., 2016, "Doped Calcium Manganites for Advanced High- Temperature Thermochemical Energy Storage," Int J Energy Res, **40**(4), pp. 280–284.

[10] Gorman, B. T., Miller, J. E., and Stechel, E. B., 2015, "Thermodynamic Investigation of Concentrating Solar Power with Thermochemical Storage," *ASME*, San Diego, CA, pp. 1–10.

[11] Jackson, G. S., Imponenti, L., Albrecht, K. J., Miller, D. C., and Braun, R. J., 2019, "Inert and Reactive Oxide Particles for High-Temperature Thermal Energy Capture and Storage for Concentrating Solar Power," Journal of Solar Energy Engineering, Transactions of the ASME, **141**(2), pp. 1–14.

[12] Babiniec, S. M., Miller, J. E., Ho, C. K., Coker, E. N., and Loutzenhiser, P. G., 2016, "Considerations for the Design of a High-Temperature Particle Reoxidation Reactor for Extraction of Heat in Thermochemical Energy Storage Systems," *ASME 2016 10th International Conference on Energy Sustainability*, pp. 1–6.

[13] Albrecht, K. J., Jackson, G. S., and Braun, R. J., 2018, "Evaluating Thermodynamic Performance Limits of Thermochemical Energy Storage Subsystems Using Reactive Perovskite Oxide Particles for Concentrating Solar Power," Solar Energy, **167**(April), pp. 179–193.

[14] Albrecht, K. J., Jackson, G. S., and Braun, R. J., 2016, "Thermodynamically Consistent Modeling of Redox-Stable Perovskite Oxides for Thermochemical Energy Conversion and Storage," Appl Energy, **165**, pp. 285–296.

[15] Schrader, A. J., Muroyama, A. P., and Loutzenhiser, P. G., 2015, "Solar Electricity via an Air Brayton Cycle with an Integrated Two-Step Thermochemical Cycle for Heat Storage Based on Co3O4/CoO Redox Reactions: Thermodynamic Analysis," Solar Energy, **118**, pp. 485–495.

[16] Klein, S. A., 2020, "F-Chart Software: EES."

[17] Miller, J. E., Babiniec, S. M., Coker, E. N., Loutzenhiser, P. G., Stechel, E. B., and Ambrosini, A., 2022, "Modified Calcium Manganites for Thermochemical Energy Storage Applications," Front Energy Res, **10**.

[18] Žukauskas, A., 1972, "Heat Transfer from Tubes in Crossflow," *Advances in Heat Transfer*, J.P. Hartnett, and T.F. Irvine, eds., pp. 93–160.

[19] Dittus, F. W., and Boelter, L. M. K., 1985, "Heat Transfer in Automobile Radiators of the Tubular Type," Int. Comm. Heat and Mass Transfer, **12**, pp. 3–22.

[20] Bell, I. H., Wronski, J., Quoilin, S., and Lemort, V., 2014, "Pure and Pseudo-Pure Fluid Thermophysical Property Evaluation and the Open-Source Thermophysical Property Library CoolProp," Ind Eng Chem Res, **53**(6), pp. 2498–2508.

[21] Whitaker, S., 1972, "Forced Convection Heat Transfer Correlations for Flow In Pipes, Past Flat Plates, Single Spheres, and for Flow in Packed Beds and Tube Bundles," AIChE Journal, **18**(2), pp. 361–371.

[22] Virtanen, P., Gommers, R., et al. 2020, "SciPy 1.0: Fundamental Algorithms for Scientific Computing in Python," Nat Methods, **17**(3), pp. 261–272.

DOI: 10.17185/duepublico/77309

DOI: 10.17185/duepublico/77309
URN: urn:nbn:de:hbz:465-20230427-142220-3